Altimeter data and ECCO2 ocean state estimates used to study the variability of Antarctic Circumpolar Current Fronts and the formation of Antarctic Intermediate Water

Victor Zlotnicki, Michael Schodlok, and Dimitris Menemenlis
Jet Propulsion Laboratory, California Institute of Technology

This work will

*** estimate interannual changes in Antarctic Circumpolar Current (ACC) frontal locations and their relation to Antarctic Intermediate Water (AAIW) formation rates,**

*** better describe and understand processes responsible for the ventilation of intermediate waters, and**

*** quantify the sensitivity of ACC frontal variability and of AAIW formation rates to changes in wind patterns.**

The proposed work will provide feedback to the ECCO2 project towards improving the representation of intermediate water formation.

In the classical view, AAIW forms in the APFZ (Tomczak and Godfrey, 1994; Speer et al., 2000), a region of high eddy activity (Meredith and Hogg, 2006) and deep winter time mixing, bounded by the Polar Front (PF) to the south and the Subantarctic Front (SAF) to the north,, while Sub Antarctic Mode Water (SAMW) forms to the north of the APFZ. A newer view connects AAIW and SAMW formation to the area between APFZ and the line of zero wind stress curl (Talley et al, 2006). AAIW is denser than SAMW and it ventilates the shallow branch of the overturning circulation through subduction. Studies dating back to Wüst (1936) revealed the hydrographic characteristics of AAIW, that is, its subsurface salinity minimum and oxygen maximum, and its spreading pathways well into the northern hemisphere. Older studies assumed the formation region to occur all around Antarctica, by the late 1970's the formation regions had been narrowed down to the South Eastern Pacific and to the Western South Atlantic (Sloyan and Rintoul, 2001); today the focus is on the South Eastern Pacific only.
In both the classical and newer views of AAIW formation, Southern Ocean fronts are the boundaries for water mass transformation. Due to the frontal dynamics (Lee et al., 2006) fronts are intimately tied to water mass formation processes.

Pioneering work by Orsi et al (1995), Belkin and Gordon (1996) described the time-averaged ACC fronts using hydrography, and pioneering work by Gille (1994) described their time variability with radar altimetry. Dong et al (2006) used 3 years of microwave sea surface temperature and showed that the seasonal cycle of ACC front latitudinal change is not zonally coherent, but it does respond to latitudinal changes in the wind stress. Sokolov and Rintoul (2007) show that the 'fronts' are made up of multuple filaments.

What has changed since then: Gille had to use a method quite sensitive to initial guess because she was fitting the differences between sea surface height and an unknown time mean. We now have two excellent estimates of the time mean dynamic topography: (1) one derives from a highly accurate, high resolution geoid, EGM2008 (N. Pavlis, 2008, from a combination of GRACE and in-situ gravity data), and an equally well sampled altimetric mean sea surface from the Danish Space Center 2008 (Anderson and Knudsen, 2008). (2) the other one derives from an optimal combination of a lower quality mean_sea_surface minus geoid, together with surface drifters (Maximenko et al, 2008)

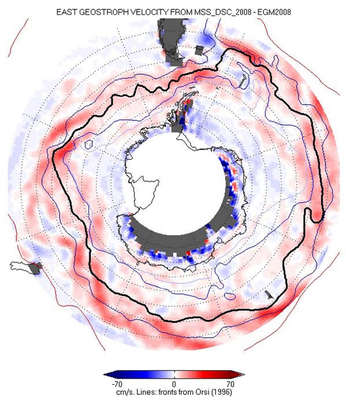

Fig 1: The zonal geostrophic velocity above is derived from a Dynamic Ocean Topography computed by D. Chambers from the difference between the DNSC 2008 mean sea surface (Anderson and Knudsen) and the EGM2008 geoid. The continuous lines show the frontal positions from Orsi et al (1996); the thick line is the Polar Front (PF), northward from the PF are the Subantarctic Front (SAF), and the Subtropical Front (STF). Southward for the PF are the Sub ACC front (SACC) and the Continental Water boundary. Note that this zonal geostrophic velocity is derived **only** from geodetic data.

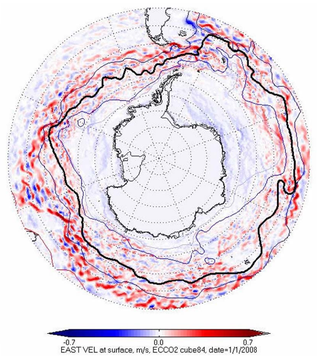

Fig 2: The ECCO2 Project (www.ecco2.org) includes several numerical model configurations and assimilation schemes. The specific data used here, labeled 'cube84', are from the cubed sphere version of the MIT ocean model, each face of the cube has 510 by 510 grid cells for a mean horizontal grid spacing of 18 km. The model has 50 vertical layers with resolution ranging from 10 m at the surface to 456 m near the bottom. A Green's function approach to data assimilation is used. Data include SSH anomalies from radar altimetry and time-mean from Maximenko and Niiler (2004), sea surface temperature from GHRSST-PP, temperature and salinity profiles from WOCE, TAO, ARGO, XBT, etc; sea ice concentration from passive microwave data, sea ice motion from radiometers,QuikSCAT, and RGPS, and sea ice thickness from ULS. The Control parameters are: * initial temperature and salinity conditions; * atmospheric surface boundary conditions; * background vertical diffusivity; * critical Richardson numbers for Large et al. (1994) KPP scheme; * air-ocean, ice-ocean, air-ice drag coefficients; * ice/ocean/snow albedo coefficients; * bottom drag and vertical viscosity. Notice the filaments, even though the model is only eddy-permitting. A solution at 1/16° exists, without data assimilation. The figure above illustrates the zonal geostrophic velocity derived from model SSH on 1/1/2008.

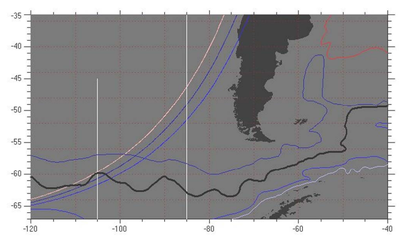

Fig 3: The map above shows the region discussed in the remainder of this Poster. The 3 TOPEX, Jason, OSTM tracks are discussed below as examples. The N-S line at LON=85°W illustrates where a cross section of model and Levitus (2001) hydrography will be shown.The line at 105°W shows the approximately position where the ACC fronts intercept these particular ground tracks.

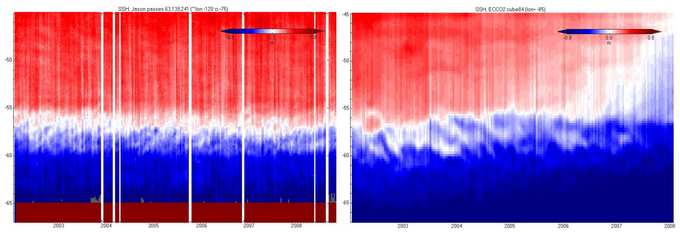

Fig 4. Both panels show SSH above the same time mean. The left panel are data along the ground tracks of Fig 3 (they were averaged at each latitude as if longitude were the same), the right panel is from ECCO2. The axes are time in years (horizontal) and latitude (vertical). Note that the ECCO2 model begins to drift away from the data around 2006; indeed, the data assimilation was done only up to 2005, and the model was run in forecast mode after that.

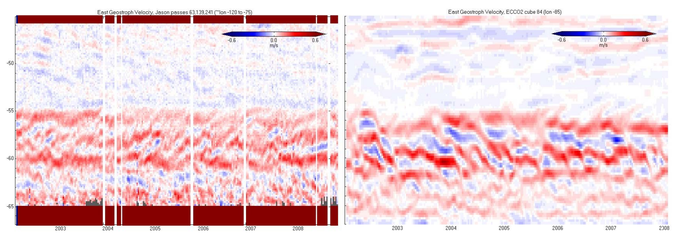

Fig 5: The zonal velocities derived from the SSH data in Fig 4. Note that despite using the time-mean DOT as a reference, the maximum zonal velocity shifts meridionally

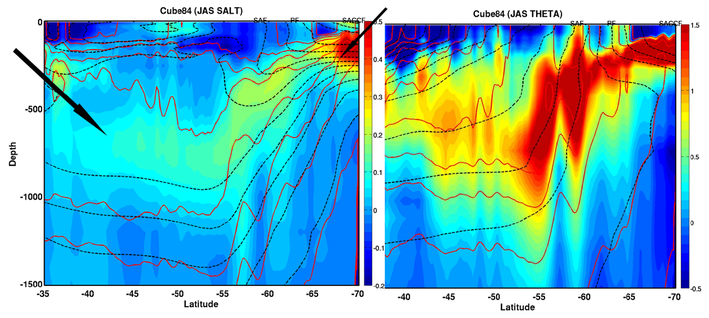

Fig 6: shows the depth-latitude sections of Salinity (left panel) and potential Temperature (right), averaged over July, August, Sept. 2003. The red lines are from ECCO, the black dashed lines from Levitus 2001 (Conkright, 2002), and the color image depicts their difference, along 85°W. Notice the AAIW layer characteristic salinity minimum in both ECCO2 and Levitus. The vertical water mass structure reflects the frontal structure. Altough WOA01 is biased towards summertime data, as winter observations are rare, AAIW formation shows in austral winter as a low salinity tongue (arrows) originating at the surface and descending to about 1000 m depth. The ECCO2 solution is too fresh in these month to produce the AAIW depicted by climatology. AAIW is being formed earlier in ECCO2, as the isohalines show, but is rather too salty and too warm. The ECCO2 isotherms show a chimney like structure indicating convection rather than subduction. The location north of the APFZ indicates Mode Water formation, rather than AAIW in ECCO2. At this stage the model does not discriminate between SAMW and AAIW water formation as such. We intend to make comparisons similar to Figure 7 against cruise (not climatological) data, for example WOCE P18 (1/1994) and P17E (12/1992).

Next steps:
* extend time series of frontal positions. COmpare to Gille's and Dong's (from SST).
* analyze time series of AAIW formation in model over the period of integration
* Formation and subduction rates in the ECCO2 solutions will be diagnosed using the methodology of Marshall et al. (1999), implemented in the MITgcm with routines by G. Maze (http://mitgcm.org/cgi-bin/viewcvs.cgi/MITgcm_contrib/gmaze_pv/)
* Additionally, dye tracer release experiments will be used to determine how Antarctic intermediate waters spread following formation and the interannual variability of formation and subduction processes. Dye will be released in the different basins, at latitudinal extents diagnosed from the time-varying locations of three ACC fronts, and the zones they delimit.

Data Quality Discussion

In addition to the science work described in the rest of this Poster, we performed some data quality assessments:
- SSB computations from short time series (see poster by Hausman and Zlotnicki)
- Jason-1 GDR-B vs Jason-1 GDR-C

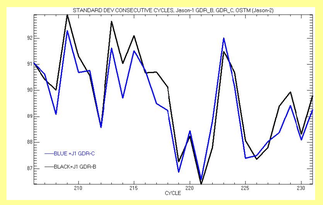

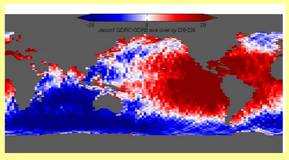

Fig A1 (left), A2 (right): A1 shows the standard deviation of **consecutive** cycle differences, using Jason-1 GDR-B and GDR-C. There has indeed been a small decrease in this error measure in going to GDR-C. However, users must be aware that there are large-scale systematic differences between GDR-B and GDR-C (Fig A2) and whatever older Topex data one may have (consistent with J1 GDR-B). Until a full reprocessing of all the data has been achieved, users may prefer to download data which has been made partially consistent, such as Remko Scharroo's RADS (http://rads.tudelft.nl)

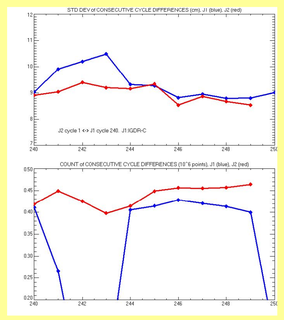

Fig A3: shows the standard deviation (top) and data count (bottom), averaged over one cycle, of consecutive cycle differences for Jason-1 IGDR (blue) and Jason-2 / OSTM (red). Notice that even this early release of OSTM data provides a higher data count and lower standard deviation (interpreted as lower overall data noise).

This work was perfomed at the Jet Propulsion Laboratory, California Institute of Technology, under contract to the National Aeronautics and Space Administration.